output power and far-field angle are, to our knowledge, the best of any monolithic 1.55 μm singlemode VCSEL to date. Singlemode CW operation was observed from −20 to 55°C. We expect to be able to reduce the threshold current and extend operation to higher temperatures with further optimisation of device design and gain offset.

© IEE 2003 *9 October 2002*
Electronics Letters Online No: 20030098
DOI: 10.1049/el:20030098

A. Hsu, D. Leonard, N. Cao, F.M. Ahedo, C. LaBounty and M.H. MacDougal (*Gore Photonics, 425 Commerce Court, Lompoc, CA 93436, USA*)

E-mail: ahsu@wlgore.com

References

1 ORTSIEFER, M., SHAU, R., ZIGLDRUM, M., BOHM, G., KOHLER, F., and AMANN, M.-C.: 'Submilliamp long-wavelength InP-based vertical-cavity surface-emitting laser with stable linear polarisation', *Electron. Lett.*, 2000, **36**, pp. 1124–1126

2 YUEN, W., LI, G.S., NABIEV, R.F., BOUCART, J., KNER, P., STONE, R.J., ZHANG, D., BEAUDOIN, M., ZHENG, T., HE, C., YU, K., JANSEN, M., WORLAND, D.P., and CHANG-HASNAIN, C.J.: 'High-performance 1.6 μm single-epitaxy top-emitting VCSEL', *Electron. Lett.*, 2000, **36**, pp. 1121–1123

3 NAKAGAWA, S., HALL, E., ALMUNEAU, G., KIM, J.K., BUELL, D.A., KROEMER, H., and COLDREN, L.A.: '1.55-μm InP-lattice-matched VCSELs with AlGaAsSb-AlAsSb DBRs', *IEEE J. Sel. Top. Quantum Electron.*, 2001, **7**, pp. 224–230

4 KARIM, A., PIPREK, J., ABRAHAM, P., LOFGREEN, D., CHIU, Y.-J., and BOWERS, J.E.: '1.55-μm vertical-cavity laser arrays for wavelength-division multiplexing', *IEEE J. Sel. Top. Quantum Electron.*, 2001, **7**, pp. 178–183

5 JAYARAMAN, V., GOODNOUGH, T.J., BEAM, T.L., AHEDO, F.M., and MAURICE, R.A.: 'Continuous-wave operation of single-transverse-mode 1310-nm VCSELs up to 115°C', *IEEE Photonics Technol. Lett.*, 2000, **12**, pp. 1595–1597

6 OHISO, Y., OKAMOTO, H., IGA, R., KISHI, K., and AMANO, C.: 'Single transverse mode operation of 1.55-μm buried heterostructure vertical-caivty surface-emitting lasers', *IEEE Photonics Technol. Lett.*, 2002, **14**, pp. 738–740

Analysis of leaky modes in circular dielectric rod waveguides

Ki Young Kim, Heung-Sik Tae and Jeong-Hae Lee

The leaky modes of dielectric rod waveguides are analysed based on the normalised phase and attenuation constants obtained using Davidenko's method. It was found that for several lower-order transverse magnetic (TM) modes, the nonphysical leaky mode, antenna mode, reactive mode, and spectral gap all existed below the cutoff frequency of the guided mode.

Introduction: A circular dielectric rod waveguide is one of the simplest guiding structures that can be used as either a waveguide or an antenna. The dispersion of its guided mode in the slow wave region is well known, whereas its leaky mode characteristics have hardly been explored below the cutoff frequency of the guided mode. In 1969, Arnbak demonstrated the existence of leaky modes in a circular dielectric rod [1] by obtaining the complex propagation constant from an approximate analysis of the characteristic equation. However, more detailed discussion about classifications of the leaky modes was unavailable at that time. Accordingly, the current Letter precisely determines the normalised complex propagation constants for the leaky mode of a dielectric rod waveguide using Davidenko's method [2]. For the several lower-order TM modes, from TM_{01} to TM_{04}, the leaky mode characteristics, such as the nonphysical leaky mode, antenna mode, reactive mode, and spectral gap are all investigated with a variation in the operating frequency from 0 to 60 GHz.

Characteristic equation and its complex root: The characteristic equation for the TM mode represents the most general feature of a dielectric rod embedded in the surrounding free space, since the characteristic equation for the TE mode is identical with that for the TM mode, except for the material constants and the hybrid mode can be represented by the linear combination of the two transverse modes. The characteristic equation of the TM mode with a time convention of $e^{j\omega t}$ is as follows:

$$\frac{\varepsilon_{r1}}{k_1}\frac{J_1(k_1 a)}{J_0(k_1 a)} - \frac{\varepsilon_{r2}}{k_2}\frac{H_1^{(2)}(k_2 a)}{H_0^{(2)}(k_2 a)} = 0 \qquad (1)$$

where J_m and H_m^2 ($m = 0, 1$) are the mth order Bessel function and the Hankel function of the second kind, respectively; ε_{r1} and ε_{r2} are the dielectric constants of the dielectric rod and free space, respectively, a is the radius of the dielectric rod, and k_1 and k_2 are the complex transverse propagation constants in the dielectric region and free space region, respectively, and are related to the normalised complex propagation constant, $\bar{\gamma}$, which is normalised with the free space wave number, k_0.

$$k_i^2 = k_0^2 \mu_{ri}\varepsilon_{ri} - \gamma^2 = k_0^2(\mu_{ri}\varepsilon_{ri} - \bar{\gamma}^2) \quad (i = 1, 2) \qquad (2)$$

The normalised complex propagation constant is composed of the normalised phase constant, $\bar{\beta}$, and normalised attenuation constant, $\bar{\alpha}$

$$\bar{\gamma} = \frac{\gamma}{k_0} = \frac{\beta - j\alpha}{k_0} = \frac{\beta}{k_0} - j\frac{\alpha}{k_0} = \bar{\beta} - j\bar{\alpha} \qquad (3)$$

Davidenko's method is used to determine both the normalised phase and the normalised attenuation constants. The resulting normalised phase and normalised attenuation constants are substituted into (1) and checked based on the accuracy of the returned value compared with zero, achieving tolerances under 10^{-10} for both the real and imaginary parts.

Results and discussion: Figs. 1 and 2 show the normalised phase and normalised attenuation constants of a dielectric rod waveguide for the leaky modes and guided modes, respectively. Two design parameters, i.e. the dielectric constant and radius of the dielectric rod, were arbitrarily chosen to be 5.0 and 5.0 mm, respectively. The cutoff frequencies of the guided mode were 11.48, 26.36, 41.32, and 56.30 GHz for the TM_{01}, TM_{02}, TM_{03}, and TM_{04} modes, respectively, and below these cutoff frequencies, nonzero values for the normalised attenuation constants were introduced. Fig. 3 shows on an enlarged scale the normalised phase constant when the value of the normalised phase constant was near unity. In Fig. 1, at low frequencies near zero, the normalised phase constants exceeded unity; this regime has no physical meaning [3], and the upper limits of the nonphysical regime were 3.51, 1.98, 1.95, and 1.94 GHz for the TM_{01}, TM_{02}, TM_{03}, and TM_{04} modes, respectively, shifting towards lower frequencies with a higher mode. Above these frequency limits, as seen in Fig. 1, the normalised phase constants decreased to a minimum point, then increased again up to unity. This regime corresponds to the physical leaky mode [4], as the higher mode had the lower value for the minimum point of the normalised phase constant, at which point the frequencies shifted to a higher frequency. This physical leaky mode regime can be divided into two distinct regions an antenna mode region ($\bar{\beta} < 1$, $\bar{\beta} > \bar{\alpha}$) and reactive mode region ($\bar{\beta} < 1$, $\bar{\beta} > \bar{\alpha}$) [5]. Note that the TM_{01} mode did not have a reactive mode region, since the frequency with the normalised phase constant equal to the normalised attenuation constant lay within the nonphysical leaky mode region. The reactive mode regions for the TM_{02}, TM_{03}, and TM_{04} modes ranged from 1.98 to 17.15 GHz (15.17 GHz in width), 1.95 to 30.57 GHz (28.62 GHz), and 1.94 to 43.93 GHz (41.99 GHz), respectively, whereas the antenna mode regions ranged from 17.15 to 20.27 GHz (3.12 GHz in width), 30.57 to 35.76 GHz (5.19 GHz), and 43.93 to 51.17 GHz (7.24 GHz) for the TM_{02}, TM_{03}, and TM_{04} modes, respectively. The widths of both the reactive mode region and the antenna mode region increased with an increase in the mode order. As the operating frequency approached a frequency higher than the antenna mode region, the normalised phase constants exceeded unity again, as in the nonphysical leaky mode region, refer to Fig. 3. This region was also a leaky mode region with no physical meaning, and called the spectral gap region, which ranged from 20.27 to 22.84 GHz (2.57 GHz in width), 35.76 to 39.13 GHz (3.37 GHz), and 51.17 to 54.70 GHz (3.53 GHz) for the TM_{02}, TM_{03}, and TM_{04} modes, respectively, plus the width increased with a higher mode. The TM_{01} mode had no spectral gap region (and no reactive mode region), and only one antenna mode region ranged from 3.51 to 11.48 GHz (7.97 GHz in width), indicating that the leaky mode of the TM_{01} mode differs from that of other high order modes. The remaining portion of the leaky mode region was another antenna mode region above the spectral gap region in frequency, ranging from 22.84 to 26.36 GHz (3.52 GHz in width), 39.13 to 41.32 GHz (2.19 GHz), and 54.70 to 56.30 GHz (1.60 GHz) for the TM_{02}, TM_{03}, and TM_{04} modes, respectively. The widths of the second antenna mode regions tended to decrease with an increase in the mode order. The upper limit frequency of this range was the same as the cutoff frequency of the guided mode. In other guiding structures, such as an NRD guide [4] or partially dielectric-loaded open guiding structure [6], the normalised attenuation constants become zero at the frequency with the maximum normalised phase constants within the spectral gap region. However, the normalised attenuation constant of the dielectric rod became zero at this frequency, i.e. the upper limit of the second antenna mode region or cutoff of the guided mode. Hence, it was observed that the spectral gap region was not always consistent with the transition region between the guided mode and the leaky mode in the case of a dielectric rod waveguide. However, it was unclear whether or not this discrepancy was induced from the circular geometry of the rod waveguide or the all-dielectric boundary of the rod waveguide, when compared with a NRD guide or partially dielectric-loaded open guiding structure.

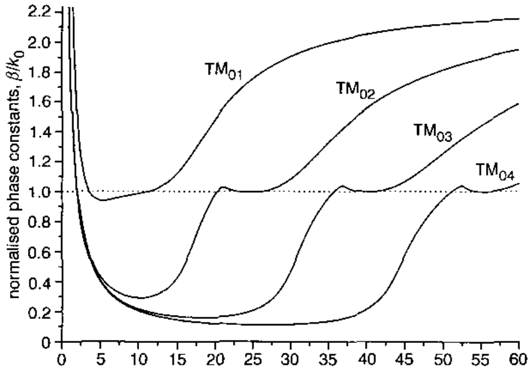

Fig. 1 *Normalised phase constant*

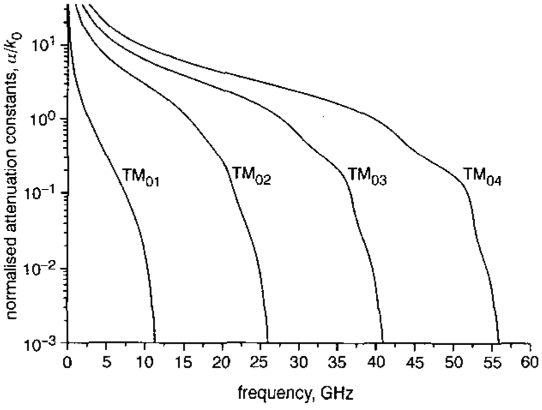

Fig. 2 *Normalised attenuation constant*

Conclusion: The leaky mode characteristics of circular rod dielectric waveguides were analysed from normalised complex propagation constants precisely determined using Davidenko's method. For the several lower-order TM leaky modes, the nonphysical leaky mode regions, antenna mode regions, reactive mode regions, and spectral gap regions were all investigated relative to the operating frequency.

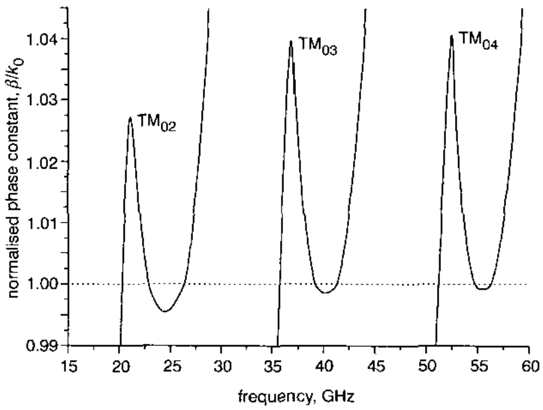

Fig. 3 *Normalised phase constant on enlarged scale*

Acknowledgments: The authors would like to thank Young Ki Cho for his valuable comments. This work was supported by grant No. R01-2000-00261 from the Basic Research Program of the Korea Science and Engineering Foundation.

14 October 2002

Electronics Letters Online No: 20030111

DOI: 10.1049/el:20030111

Ki Young Kim and Heung-Sik Tae (*School of Electronic and Electrical Engineering, Kyungpook National University, Daegu 702-701, Korea*)

E-mail: hstae@ee.knu.ac.kr

Jeong-Hae Lee (*Radio Science and Communication Engineering, Hongik University, Seoul 121-791, Korea*)

References

1 ARNBAK, J.: 'Leaky waves on dielectric rod', *Electron. Lett.*, 1969, **5**, (3), pp. 41–42

2 HEJASE, H.A.N.: 'On the use of Davidenko's method in complex root search', *IEEE Trans. Microw. Theory Tech.*, 1993, **41**, (1), pp. 141–143

3 LAMPARIELLO, P., FREZZA, F., SHIGESAWA, H., TSUJI, M., and OLINER, A.A.: 'A versatile leaky-wave antenna based on stub-loaded rectangular waveguide. Part I—Theory', *IEEE Trans. Microw. Theory Tech.*, 1998, **46**, (7), pp. 1032–1041

4 NALLO, C.D., FREZZA, F., GALLI, A., LAMPARIELLO, P., and OLINER, A.A.: 'Properties of NRD-guide and H-guide higher-order modes physical and nonphysical ranges', *IEEE Trans. Microw. Theory Tech.*, 1994, **42**, (12), pp. 2429–2434

5 ZENG, X., XU, S., WU, K., and LUK, K.: 'Properties of guided modes on open structures near the cutoff region using a new version of complex effective dielectric constant', *IEEE Trans. Microw. Theory Tech.*, 2002, **50**, (5), pp. 1417–1424

6 LAMPARIELLO, P., FREZZA, F., and OLINER, A.A.: 'The transition region between bound-wave and leaky-wave ranges for a partially dielectric-loaded open guiding structures', *IEEE Trans. Microw. Theory Tech.*, 1990, **38**, (12), pp. 1831–1836

Bandpass filter using microstrip ring resonators

Q.S. Wu, Q. Xue and C.H. Chan

A new ring resonator with enhanced coupling is proposed. For a 5.2 GHz resonator, $|S_{21}|$ of the second resonant mode is 12 dB below that of the first mode. Based on this new structure, a bandpass filter is constructed. The insertion loss is 0.2 dB better and out-of-band suppression at 150 MHz offset is 7 dB better than those of the generic coupled-line filter and the size is 21% smaller.

Introduction: The microstrip ring resonator has been widely used to measure the dispersion, phase velocity, and effective dielectric